International Journal of Adhesion & Adhesives 55 (2014) 155–160

Contents lists available at ScienceDirect

International Journal of Adhesion & Adhesives

journal homepage: www.elsevier.com/locate/ijadhadh

A tapered bondline thickness double cantilever beam (DCB) specimen geometry for combinatorial fracture studies of adhesive bonds

Shantanu R. Ranade [a], Youliang Guan [b], Donatus C. Ohanehi [b], John G. Dillard [c], Romesh C. Batra [b], David A. Dillard [b,*]

[a] Macromolecules and Interfaces Institute, Virginia Polytechnic Institute and State University, Blacksburg, VA 24061, United States
[b] Department of Biomedical Engineering and Mechanics, Virginia Polytechnic Institute and State University, Blacksburg, VA 24061, United States
[c] Department of Chemistry, Virginia Polytechnic Institute and State University, Blacksburg, VA 24061, United States

ARTICLE INFO

Article history:
Accepted 20 July 2014
Available online 20 August 2014

Keywords:
Adhesives
Structural adhesives
Bondline thickness
DCB
Fracture
Epoxy adhesives
Combinatorial characterization
Fracture energy
SENB
Plastic zone

ABSTRACT

The characterization of fracture energy (G_{Ic}) of an adhesive joint as a function of bondline thickness requires multiple specimens covering a range of bondline thicknesses. In this work, DCB specimens with linearly increasing or decreasing bondline thickness were studied for their feasibility to determine fracture energy as a function of bondline thickness. In a combinatorial characterization sense, this approach explores the possibility to characterize the effect of bondline thickness on fracture energy through fewer tests than those required for a "one at a time" characterization approach, thus offering a significant reduction in characterization times. Fracture energies were characterized under mode I loading conditions using corrected beam theory. The results obtained from linearly increasing or decreasing bondline thickness specimens showed good agreement with those obtained from specimens with a range of constant bondline thicknesses.

1. Introduction

The effect of bondline thickness (t), on adhesive joint performance has been the subject of considerable research, with many studies showing quite significant differences in resistance to failure as a function of the adhesive bondline thickness[1–13]. It has been observed, as shown schematically in Fig. 1 for toughened epoxy adhesive systems, that the fracture energy of an adhesive joint shows complex dependence upon the bondline thickness, with fracture energy values passing through a maximum at a certain bondline thickness t_m [1–3,10].

It has been suggested that such behavior, for a toughened adhesive system, is due to varying amounts of plastic deformation that develop ahead of the crack tip. In the fracture of monolithic materials, the radius of the plastic zone (r_p) developing at the crack tip often affects the resulting fracture energy. For small adhesive bondline thickness, $t < t_m$, the development of the plastic zone at the crack tip is restricted due to the presence of stiff, high yield strength adherends. Thus the adhesive fracture energy decreases with a decrease in the bondline thickness for $t < t_m$. As shown in Fig. 2(a), at $t = t_m$, the plastic zone ahead of the crack tip is fully developed with the diameter of the plastic zone ($2r_p$) normal to the plane of the crack being nearly equal to the bondline thickness, which results in a maximum fracture energy value for a double cantilever beam (DCB) specimen bonded with a given adhesive.

It has been reported that due to constraints imposed by stiff adherends, local tensile stresses ahead of the crack tip act over longer distances, thus leading to plastic zone size being significantly longer in length in joints than those in bulk adhesive specimens [3,14,15]. In Fig. 1 at bondline thicknesses $t > t_m$, the constraint due to the presence of stiff adherends decreases, thus decreasing the length of the plastic zone and resulting in lower fracture energy values compared to the fracture energy at $t = t_m$. Similar observations have been reported based on studies using finite element methods [7,8]. Cooper et al. conducted finite element analysis of tapered double cantilever beam (TDCB) joints with several bondline thicknesses, using a Dugdale-type cohesive zone model (CZM) to simulate mode I fracture in an adhesive joint [9]. Martiny et al. used a model based on a critical maximum principal stress at a critical distance ahead of a crack tip as a failure criterion to study the variation of the fracture energy with the bondline thickness [10,16]. It has been observed for toughened epoxy adhesive systems that the fracture energy vs. bondline thickness trends and the maximum in the fracture energy value also depend upon test variables such as the loading rate and

* Corresponding author. Tel.: +1 5 4 0 231 4714.
E-mail address: dillard@vt.edu (D.A. Dillard).

http://dx.doi.org/10.1016/j.ijadhadh.2014.08.006
0143-7496/

the test temperature. It was also observed that at a given loading rate, test temperature changes in joint width altered trends for the fracture energy as a function of the bondline thickness [1].

In light of the dependence of the fracture energy on the bondline thickness and to maintain high quality of joints, the aircraft industry has long used techniques that tightly control the bondline thickness for critical structural joints. The use of supporting scrim cloth layers, for example, resists the flow of viscous adhesives and can result in good bondline thickness control [17]. However, in some applications, tolerances over bondline thickness are less strict, such as in the mass-produced automotive industry. The very large size and complex shapes involved in wind turbine blade assembly lead to an even wider range of bondline thicknesses, which may be many millimeters thick, much thicker than what has typically been used or recommended for structural joints. For these and other similar applications, an understanding of adhesive joint performance as a function of bondline thickness is critical. This typically requires characterizing the fracture energy using multiple DCB specimens, with each specimen having a constant bondline thickness. This "one at a time" characterization approach requires many specimens and significant preparation, testing, and analysis effort.

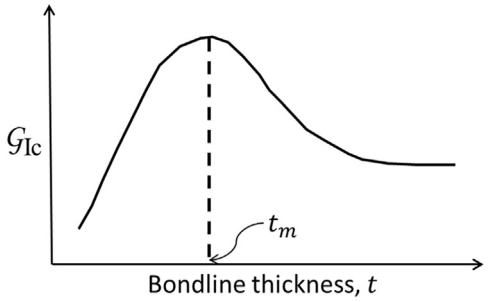

Fig. 1. Schematic representation of the effect of bondline thickness on mode I fracture energy of a toughened epoxy adhesive DCB specimen.

In a combinatorial characterization sense, the approach outlined in this study aims to explore the possibility of characterizing the effect of the bondline thickness on the fracture energy through fewer tests and in less time than those required for "one at a time" bondline thickness characterization approach. In this study the feasibility of using double cantilever beam (DCB) specimens with either increasing or decreasing bondline thickness (Fig. 3) has been assessed to determine the fracture energy as a function of the bondline thickness. An estimate of the plastic zone size in mode I plane strain conditions for bulk adhesive specimens was obtained through single edge notch bend (SENB) tests and the plastic zone size was then compared to t_m measured (Fig. 1) in DCB tests.

2. Experimental work

2.1. DCB tests

DCB test specimens were prepared using 6061-T6511 aluminum adherends, having dimensions of 305 mm × 25.4 mm × 12.7 mm (length × width × thickness). Circular holes were drilled at one end of each aluminum bar to accommodate 6.4 mm diameter loading pins. The adherends were then abraded with #220 sandpaper and exposed to a base-acid surface treatment, which consisted of placing aluminum bars in 10% (wt/wt) NaOH solution for 10 min, rinsing with deionized (DI) water and placing them in HNO_3:H_2O = 1:1 (vol/vol) for 2 to 3 min or until the surfaces regained a white metallic appearance. The adherends were then rinsed again with DI water, and placed in an oven heated to 110 °C for about 2 h to remove moisture absorbed on the surface. Two types of specimens were prepared. The first type of specimens had several constant adhesive bondline thicknesses (six specimens with bondline thicknesses of 0.02 mm, 0.77 mm, 1.7 mm, 1.87 mm, 2.26 mm, and 4.52 mm); the second type of specimens consisted of 10 either linearly increasing or linearly decreasing

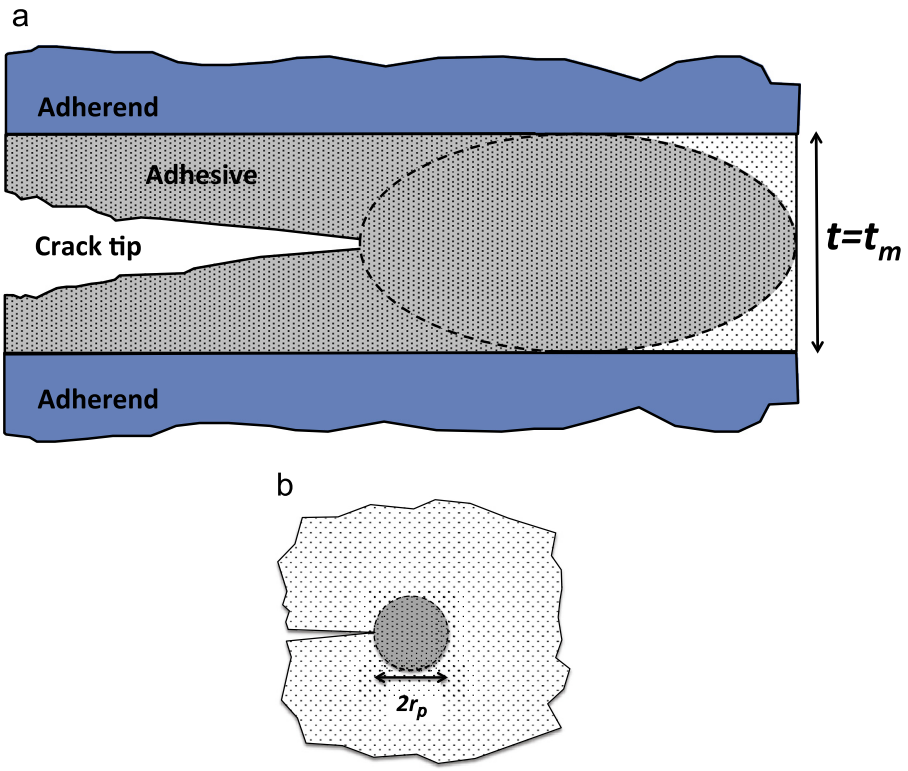

Fig. 2. Schematic sketch of the plastic zone developed at a crack tip in (a) an adhesive joint at bondline thickness $t = t_m$ [1], and (b) in a monolithic elastic–plastic material.

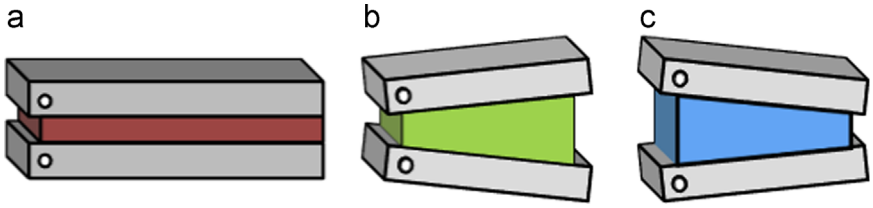

Fig. 3. Exaggerated schematic diagrams of DCB specimens with adhesive bondline thickness (a) constant, (b) increasing, and (c) decreasing.

bondline thickness specimens, depending upon which end was drilled for the loading pins and the direction in which the subsequent debond propagated. Exaggerated schematic sketches of the three types of specimens are shown in Fig. 3. Commercially available LORD™ 320/322 structural epoxy adhesive was used to bond the aluminum adherends. Before bonding, each pair of adherends was marked on the outer (non-bonding) surface at five locations spaced at approximately equal intervals along the specimen length using a permanent marker and the thickness of the adherends was measured at these locations. The adhesive was then applied on one of the adherends and the adherends were clamped together at both ends while maintaining the alignment of the adherends. The desired bondline thicknesses were achieved by placing spacers of appropriate thickness at each end of the specimen. Due to the highly viscous nature of the adhesive, no confinement was necessary to prevent the adhesive from flowing out of the bondline. Specimens were then cured for 14 h at room temperature, followed by a post-cure at 60 °C for 3 h. All adhesive joint and bulk adhesive specimens used in this study were cured at same conditions. Based on dynamic mechanical analysis measurements (temperature sweep, 1Hz), the glass transition temperature of bulk adhesive specimens was 85°C for the mentioned curing conditions. After bonding, the total thicknesses of the bonded specimens were measured at the marked locations on the adherends and the bondline thickness at marked locations was calculated by subtracting adherend thicknesses from the total thickness of the specimens. For linearly increasing or linearly decreasing bondline thickness specimens, the distances between marked locations and drilled holes were measured, and the bondline thickness values at the first and the last marked location from the drilled holes were plotted as a function of the distance from the loading holes. A straight line was fitted through the points, and an expression for the bondline thickness as a function of the distance from the drilled holes was obtained. This expression was used to determine the bondline thickness at each crack length. Prior to conducting the tests, typewriter correction fluid was applied on the bondline to facilitate observations of the crack tip. Paper rulers were affixed to the specimens to help measure crack growth. The DCB tests were carried out at room temperature (about 25 °C) in an Instron model 5500R in mode I conditions at a total crosshead rate of 0.1 mm/min. The mode I fracture energies were calculated using corrected beam theory (CBT) (Eq. 1) [18, 19].

$$\mathcal{G}_{Ic} = \frac{3P\delta}{2B(a+\hat{a})}F \tag{1}$$

where $\mathcal{G}_{Ic}$ is mode I fracture energy; a is crack length; P is load measured by load cell at crack length, a; δ is crosshead displacement at a crack length, a; F is large displacement correction; B is width of the specimen and $\hat{a}$ is the crack length correction for a beam that is not perfectly built in.

2.2. Three point bend tests

The single edge notch bend (SENB) tests were used to calculate the plane strain fracture toughness (K_{Ic}) of the bulk adhesive specimens, following the ASTM D 5045-99 standard. Bulk adhesive specimens were cast using silicone molds. The SENB specimens had dimensions of about 57.1 mm × 12.7 mm × 6.3 mm (length × width × thickness). Specimens were pre-cracked by driving a fresh, sharp razor blade by gentle tapping such that the crack tip was a few millimeters ahead of the razor blade tip. Due to the lack of distinguishing features on the fractured surfaces of the SENB specimens, it was not possible to unambiguously measure the length of the pre-crack from fractured specimens. Crack lengths were measured using high-resolution images of the pre-cracked specimens and digital image analysis software. Pre-cracked specimens were then mounted crack down on a 3-point bend fixture in an Instron model 5500R and loaded at a constant crosshead rate of 0.1 mm/min. All three point bend tests were carried out at room temperature (about 25 °C). The distance between the supporting rollers in the 3-point bend fixture was 4 times the width of the specimens. Plane strain fracture toughness values were calculated as per ASTM D 5045-99 standard, utilizing tensile yield strength ($\sigma_{y\ tensile}$) values estimated from compression tests, as described in the next section [1]. The plane stress plastic zone size, r_p, was estimated using the following expression [20]:

$$r_p = \frac{1}{2\pi}\left(\frac{K_{IC}}{\sigma_{ytensile}}\right)^2 \tag{2}$$

2.3. Compression tests

Dogbone specimens were cast using silicone molds. When tested in tension to obtain tensile yield strength, specimens failed in a brittle manner, precluding the use of tensile tests for obtaining the tensile yield strength values. Similar behavior has been reported for a toughened epoxy adhesive system when tested in tension [1]. For a toughened epoxy system, it has been reported that the tensile yield strength equals nearly 0.75 times the compressive yield strength [1]. For compression tests, three cylindrical specimens were cast and cured at conditions same as those of the DCB and the SENB tests. Specimens were then machined to a height/diameter ratio between 2 and 1.5. The three specimens had a diameter in the range of 10.16 mm to 15.24 mm. The specimens were loaded between non-lubricated polished steel plates in an Instron 5500R test frame at 0.1 mm/min. The load values were converted into the nominal axial stress by dividing the load by the original cross-sectional area of the specimen. The change in the specimen length was obtained through crosshead movement and converted to the average axial strain by dividing it by the original specimen length. Compressive yield strength ($\sigma_{y\ comprresion}$) was calculated from the stress–strain curves by using 1% strain offset. Compressive modulus values were obtained from the slope of the linear part of the stress–strain curve. Compressive stress vs. compressive strain curves corrected for a toe region (artifact caused by take up of slack, alignment or seating of the specimen) are shown in Fig. 4. Guidelines from ASTM D 695 – 02a standard were used to compensate for the toe region in the compressive stress vs. compressive strain curves.

3. Results and discussion

The fracture energy vs. the crack length data for DCB specimens having a constant bondline thickness is shown in Fig. 5. It was found that as the crack propagated along the length of a specimen,

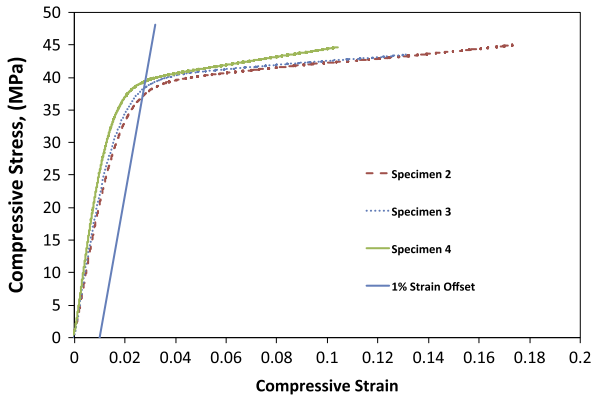

Fig. 4. Engineering compressive axial stress vs. compressive axial strain curves from compression tests.

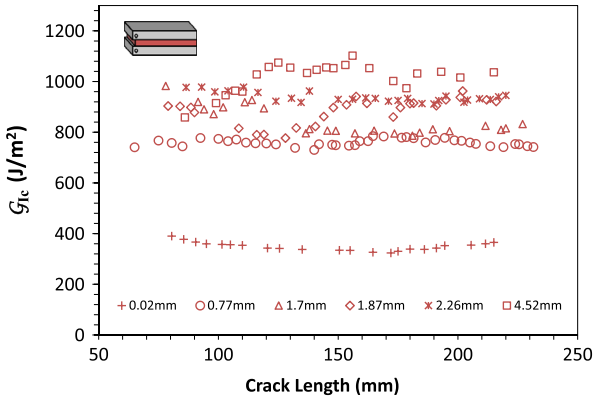

Fig. 5. Variation of mode I fracture energy with crack length for DCB specimens with constant bondline thickness.

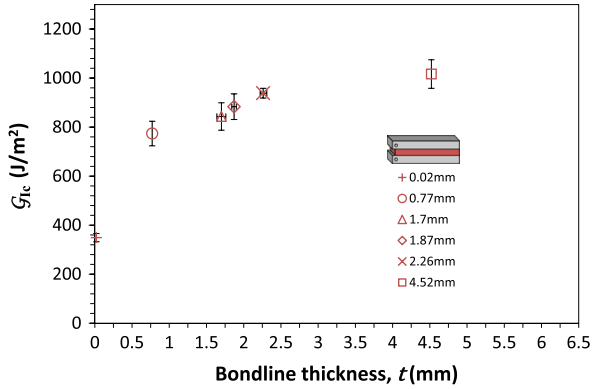

Fig. 6. Variation of mode I fracture energy with bondline thickness for DCB specimens having a constant bondline thickness.

the fracture energy remained essentially constant (within ± 10% of the average value). Similar trends were observed when fracture energies were calculated using the experimental compliance method. Fracture energy values (based on CBT) from a specimen were then averaged and plotted as a function of the bondline thickness. These plots are shown in Fig. 6. A horizontal error bar for a given data point, visible in Fig. 6, indicates the maximum and the minimum adhesive bondline thickness values measured during thickness measurements at several locations for a given DCB specimen. A vertical error bar for a given data point shows the ± 1 standard deviation of the fracture energy values for a given specimen. From results depicted in Fig. 6, it can be observed that for the adhesive system used in this study, fracture energies tend to increase with an increase in the bondline thickness up to about 2 mm and then essentially remain constant out to the maximum bondline thickness of about 4 mm.

The variation of the fracture energy with the bondline thickness for linearly increasing, linearly decreasing and constant bondline thickness DCB specimens is shown in Fig. 7. Eight DCB specimens were prepared, four of which had linearly increasing bondline thickness covering a range of 0.25 to 6.12 mm in four intervals (0.25 to 0.69 mm, 0.9 to 1.96 mm, 1.85 to 4.02 mm, 3.16 to 6.12 mm). The remaining four specimens had linearly decreasing bondline thicknesses covering a range of 6.22 mm to 0.22 mm in four intervals (6.22 to 3.11 mm, 4.18 to 1.79 mm, 2.16 to 0.88 mm, 0.65 to 0.22 mm) (Fig. 7). These bondline thickness ranges were covered in multiple intervals due to geometric restrictions where adherends begin to touch each other at the narrow ends of the specimens for a large thickness interval. Some successive intervals had a small overlap in order to characterize the fracture energy at a given bondline thickness via multiple specimens. It was observed that data from eight linearly increasing and linearly

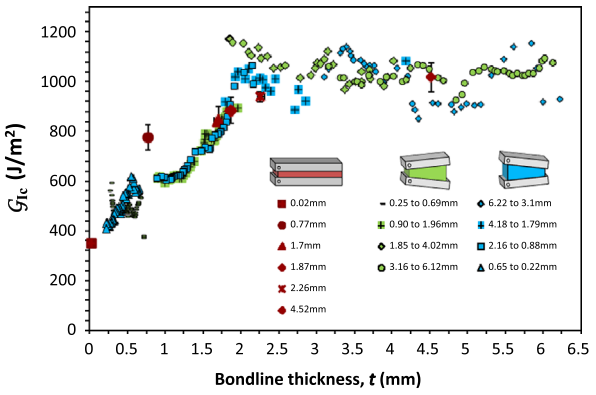

Fig. 7. Comparison of variation in the mode I fracture energy with bondline thickness between specimens with constant bondline thickness and specimens with linearly increasing and linearly decreasing bondline thickness.

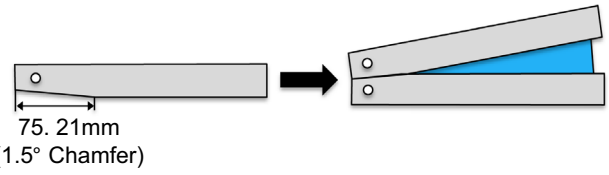

Fig. 8. Exaggerated schematic representation of a DCB specimen with modified geometry to accommodate large intervals of bondline thickness.

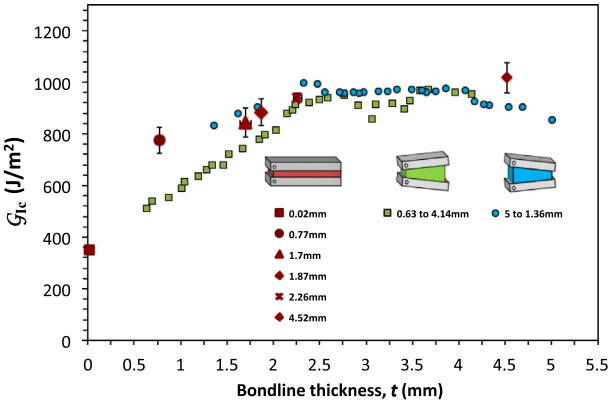

Fig. 9. Comparison of variation in the mode I fracture energy with bondline thickness between specimens having constant bondline thickness and specimens having linearly increasing and linearly decreasing bondline thickness.

Table 1

	Compressive modulus (GPa)	Compressive yield strength [a] (MPa)	Tensile yield strength[b] (MPa)	K_{Ic} (MPa $m^{0.5}$)	Plastic zone diameter[c], $2r_p$ (mm)
Average	2.45	37.8	28.3	1.16	0.51
Standard deviation	0.32	0.63	0.47	0.15	0.13

[a] Calculated using 1% offset.
[b] Equal to 0.75 (yield strength in compression) [1].
[c] Calculated using Eq. (2).

decreasing bondline thickness specimens showed good agreement with the data from constant bondline thickness specimens. A larger deviation was observed for the data obtained from a specimen with the constant bondline thickness of 0.77 mm, though the reason for this is unknown. It was also observed that data obtained from multiple specimens with overlapping thickness ranges showed good agreement with each other.

In order to test larger bondline thickness intervals using a single specimen, two DCB specimens with a modified geometry were prepared. In these specimens part of the adherend faces were chamfered to accommodate a steeper taper angle (about 3°) (Fig. 8). In the case of DCB tests with non-chamfered adherends the bondline thickness taper angle was in the range of 0.1° to 1.7°. One chamfered DCB specimen had an increasing bondline thickness, covering a bondline thickness range from 0.63 mm to 4.14 mm, and the other specimen had a decreasing bondline thickness, covering a bondline thickness range from 5 mm to 1.36 mm. It was observed that the data obtained from these specimens showed good agreement with the data obtained from constant bondline thickness specimens (Fig. 9). It is interesting to note that these specimens had a bondline thickness gradient much larger than that in the previously tested linearly varying bondline thickness specimens, which covered a similar bondline thickness range in multiple intervals. Thus, increasing the bondline thickness gradient did not appear to affect the results obtained from these modified DCB specimens. It is important to note, however, that the taper angle is still relatively small, about 3°. Significantly steeper gradients may indeed introduce some anomalies.

For the adhesive system used in this study, no peak in the fracture energy was observed. From the test data on DCB specimens having linearly increasing, linearly decreasing and constant bondline thicknesses, it was observed that fracture energies increased until a bondline thickness of approximately 2.2 mm. Fracture energies plateaued at bondline thicknesses greater than 2.2 mm with no downward trend observed up to the maximum bondline thickness used (4.5 mm). Similar results were reported by Bascom et al. for 30% carboxy-terminated butadiene-acrylonitrile (CTBN) elastomer toughened epoxy system where fracture energy values for DCB specimens increased up to a bondline thickness of about 1 mm ($t = t_m$) and remained constant with a further increase in the bondline thickness up to 2 mm [2]. Several other studies have been reported where fracture energy increases with bondline thickness and reaches a plateau without exhibiting a peak within the investigated bondline thickness ranges [8,9,21]. Kinloch et al. have reported that the extent of decrease in the fracture energy value for a rubber toughened epoxy adhesive for $t > t_m$ was affected by the loading rate, the temperature and the width of the joint. In a more recent study based on a model developed using a critical maximum principal stress at a critical distance ahead of the crack tip as a failure criterion, Matiny et al. suggested that not all adhesives would show a peak in the fracture energy as a function of the bondline thickness. It was suggested that the occurrence of a peak in the fracture energy vs. the bondline thickness curve depended upon parameters such as the modulus of the adhesive, the power law hardening exponent for the adhesive and the critical maximum principal stress ahead of the crack tip at a critical distance [10].

As mentioned earlier, it has been reported that the fracture energy of toughened epoxy adhesive joints increases up to a particular bondline thickness, which often corresponds with the plastic zone diameter ($2r_p$) measured using bulk adhesive specimens. In some of these studies plane stress conditions were considered for estimating the plastic zone diameter where it was suggested that the dissipation mechanisms, e.g. cavitation in typical rubber toughened structural epoxy adhesives, may lead to plane stress conditions near the crack tip region. Though, it should be noted that in adhesive joints, plastic zone shape and size would be more complex due to constraints imposed by the adherends and change in stress state from plane stress to plane strain through the width of the specimen [14,22,23]. The plane stress plastic zone diameter in a bulk adhesive specimen can be predicted using Eq. (2). In Table 1 we have listed average plane strain fracture toughness obtained from the SENB tests, results from compression tests, and average plane stress plastic zone diameter calculated using Eq. (2). It was observed that for the adhesive system and geometry used in this study, the plane stress plastic zone diameter estimated from bulk adhesive specimens did not correlate well and was about one-fourth the bondline thickness value of about 2.2 mm (t_m) for either constant or tapered bondline thickness DCB specimens, where fracture energy appears to reach a plateau.

4. Conclusions

This study proposes and demonstrates the use of a DCB specimen with a linearly varying bondline thickness as a potential combinatorial specimen for characterizing the effect of bondline thickness on fracture energy. For the adhesive system used in this study, data from linearly increasing and linearly decreasing bondline thickness specimens generally showed good agreement with that from constant bondline thickness specimens. It was observed that a single DCB specimen with a linearly increasing or linearly decreasing bondline thickness could provide significant insight into the effect of the fracture energy on the bondline thickness. This will result in a decrease in the testing time and effort needed to study the effect of the bondline thickness on the fracture energy of a toughened epoxy adhesive system. Concerns would be raised, however, if the bonds exhibit a clear R-curve behavior, which could obscure the results of this combinatorial specimen configuration.

Acknowledgments

We would like to thank the National Science Foundation (NSF/CMMI Award no. 0826143) for funding this project as well as LORD™ Corporation (Cary, NC) for supplying adhesives needed for this work

References

[1] Kinloch AJ, Shaw SJ. The fracture resistance of a toughened epoxy adhesive. J Adhes 1981;12:59–77 (1981/05/01).

[2] Bascom WD, Cottington RL, Jones RL, Peyser P. The fracture of epoxy- and elastomer-modified epoxy polymers in bulk and as adhesives. J Appl Polym Sci 1975;19:2545–62.
[3] Hunston DL, Kinloch AJ, Wang SS. Micromechanics of fracture in structural adhesive Bonds. J Adhes 1989;28:103–14 (1989/06/01).
[4] Mostovoy S, Ripling EJ. Effect of joint geometry on the toughness of epoxy adhesives. J Appl Polym Sci 1971;15:661–73.
[5] Mostovoy S, Ripling EJ, Bersch CF. Fracture toughness of adhesive joints. J Adhes 1971;3:125–44 (1971/11/01).
[6] Chai H. On the correlation between the mode I failure of adhesive joints and laminated composites. Eng Fract Mech 1986;24:413–31.
[7] Azari S, Papini M, Spelt JK. Effect of adhesive thickness on fatigue and fracture of toughened epoxy joints – Part II: analysis and finite element modeling. Eng Fract Mech 2011;78:138–52.
[8] Azari S, Papini M, Spelt JK. Effect of adhesive thickness on fatigue and fracture of toughened epoxy joints – Part I: experiments. Eng Fract Mech 2011;78:153–62.
[9] Cooper V, Ivankovic A, Karac A, McAuliffe D, Murphy N. Effects of bond gap thickness on the fracture of nano-toughened epoxy adhesive joints. Polymer 2012;53:5540–53.
[10] Martiny P, Lani F, Kinloch AJ, Pardoen T. A maximum stress at a distance criterion for the prediction of crack propagation in adhesively-bonded joints. Eng Fract Mech 2013;97:105–35.
[11] Lee D-B, Ikeda T, Miyazaki N, Choi N-S. Effect of bond thickness on the fracture toughness of adhesive joints. J Eng Mater Technol 2004;126:14–8.
[12] Mall S, Ramamurthy G. Effect of bond thickness on fracture and fatigue strength of adhesively bonded composite joints. Int J Adhes Adhes 1989;9:33–7.
[13] Lee D-B, Ikeda T, Miyazaki N, Choi N-S. Fracture behavior around a crack tip in rubber-modified epoxy adhesive joint with various bond thicknesses. J Mater Sci Lett 2003;22:229–33 (2003/02/01).
[14] Wang SS, Mandell JF, McGarry FJ. An analysis of the crack tip stress field in DCB adhesive fracture specimens. Int J Fract 1978;14:39–58 (1978/02/01).
[15] Ikeda T, Yamashita A, Lee D, Miyazaki N. Failure of a ductile adhesive layer constrained by hard adherends. J Eng Mater Technol 2000;122:80–5.
[16] Martiny P, Lani F, Kinloch AJ, Pardoen T. A multiscale parametric study of mode I fracture in metal-to-metal low-toughness adhesive joints,. Int J Fract 2012;173:105–33 (2012/02/01).
[17] Aglan H, Abdo Z, Shroff S. Fracture and fatigue behavior of scrim cloth adhesively bonded joints with and without rivet holes. J Adhes Sci Technol 1995;9:177–97 (1995/01/01).
[18] Blackman BRK, Kinloch AJ, Paraschi M, Teo WS. Measuring the mode I adhesive fracture energy, GIC, of structural adhesive joints: the results of an international round-robin. Int J Adhes Adhes 2003;23:293–305.
[19] I. O. f. Standardization, "Adhesives — Determination of the mode 1 adhesive fracture energy of structural adhesive joints using double cantilever beam and tapered double cantilever beam specimens," ISO 25217:2009,Switzerland.
[20] Broek D. Elementary engineering fracture mechanics. Alphen aan den Rijn: Sijthoff & Noordhoff; 1978.
[21] Kawashita LF, Kinloch AJ, Moore DR, Williams JG. The influence of bond line thickness and peel arm thickness on adhesive fracture toughness of rubber toughened epoxy–aluminium alloy laminates. Int J Adhes Adhes 2008;28:199–210.
[22] SR Ranade, Performance and Durability of Adhesive Joints, [Ph. D.], Macromolecular Sci. and Eng., Virginia Polytechnic Institute and State University, Blacksburg,VA, USA, To be published.
[23] SR Ranade, Y Guan, D Ohanehi, J Dillard, RC Batra, and DA Dillard, A tapered bondline thickness Double Cantilever Beam (DCB) specimen geometry for combinatorial fracture studies of adhesive bonds. In: Proceedings of the meeting of the Adhesion Society presented at the, Daytona, USA, 2013.